

Construction of Fast and Accurate 2D Bijective Rigid Transformation

Stéphane Breuils¹[0000-0002-8636-4977], David Coeurjolly²[0000-0003-3164-8697],
and Jacques-Olivier Lachaud¹[0000-0003-4236-2133]

¹ University of Savoie Mont-Blanc, LAMA laboratory, France

{stephane.breuils,jacques-olivier.lachaud}@univ-smb.fr

² University of Lyon, CNRS, INSA Lyon, UCBL, LIRIS, UMR5205, France

david.coeurjolly@lcnr.fr

Abstract. Preserving surfaces or volumes of digital objects is crucial when applying transformations of 2D/3D digital objects in medical images and computer vision. To achieve this goal, the digital geometry community has focused on characterizing bijective digitized rotations and reflections. However, the angular distribution of these bijective rigid transformations is far from being dense. Other bijective approximations of rigid transformations have been proposed, but the state-of-the-art methods lack the experimental evaluations necessary to include them in real-life applications. This paper presents several new methods to approximate digitized rotations with bijective transformations, including the composition of bijective digitized reflections, bijective rotation by circles and bijective rotation through optimal transport. These new methods and several classical ones are compared both in terms of accuracy with respect to Euclidean rotations, and in terms of computational complexity and practical speed in real-time applications.

1 Introduction

While rotations and translations in \mathbb{R}^d are trivial isometric and bijective transforms, their digitized cousins in \mathbb{Z}^d have attracted a lot more attention as in general, they do not preserve distances and are not bijective. Of course, direct applications of such transformations in \mathbb{Z}^d belong to the image processing or computer vision fields (template matching, object tracking...). However, the study of digitization effects of such rigid motions in \mathbb{Z}^d has led to interesting number theoretic and arithmetical results. For instance, one can characterize the set of angles for which the digitized rotation is bijective in \mathbb{Z}^2 [1], in \mathbb{Z}^3 [2], on the hexagonal lattice [3]. We can also consider rigid motions from quasi-shear transforms [4,5,6], or reflections [7,8]. For specific applications, we can even look for an approximation of the rotation preserving the homotopy for subsets of \mathbb{Z}^2 [9].

In this article, we follow this line of previous works focusing on a more practical question in \mathbb{Z}^2 : for a given rotation angle, what is the best discrete bijective

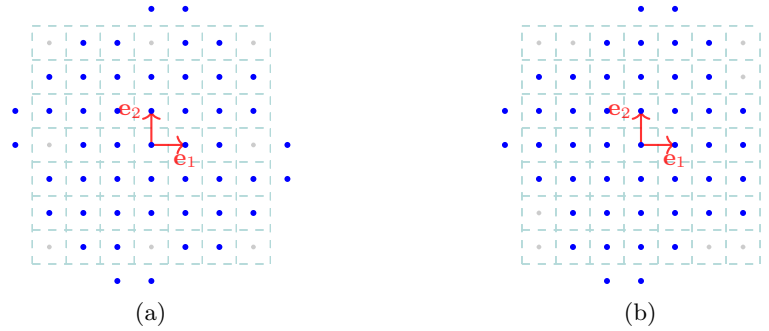


Fig. 1: 2D digitized rotations of points in blue. The digitized rotation of (a) is not bijective since it yields holes and double points whereas the rotation of (b) is bijective.

transformation we can have. More precisely, we are looking for a bijective transformation from \mathbb{Z}^2 to \mathbb{Z}^2 (or subsets of \mathbb{Z}^2) that minimizes a distance-based metric. In this context, we review existing bijective rotation approaches and propose two new approaches: the first one relies on composition of discrete reflections following [8], the second one on bijective rotation using circular annulus [10]. We demonstrate that the composition of four discrete reflections leads to the rotation with the lowest metric error. For this last approach, we also provide a lookup table that returns the best sequence of reflections (and their parameter) for a large set of angles.

2 Bijectivity of digitized rigid transformation

Let us consider rigid transformations that act on the integer lattice \mathbb{Z}^d . A digitized rigid transformation is the composition of a rigid transformation $T \in E(d)$ (element of the Euclidean group) and a rounding to the nearest integer operator $\mathcal{D} : \mathbb{R}^d \rightarrow \mathbb{Z}^d$. The rigid transformation is bijective whereas the rounding operator is not, see Figure 1.

However, there are two possibilities to ensure bijectivity of digitized rigid transformations, either

- (a) define a digitized transformation that leaves invariant lines (reflection) or circles (rotation),
- (b) or characterize rigid transformations that are bijective after digitization. Once the characterization is known, it is not difficult to approximate any rigid transformation with the "nearest" bijective one.

In the following, we only consider reflections and rotations that act on the integer lattice \mathbb{Z}^2 . We start by briefly recalling the state-of-the-art bijective approximation of rigid transformations.

2.1 Quasi-shears

The quasi-shear approach by Andres [4] consists in the discretization of the continuous horizontal and vertical shears that approximate rotation. This is a one-one point mapping thus bijective. Note that the shear method is not limited to 2D as shown by Toffoli [6] and extends well to non squared lattices as shown by [5].

2.2 Reflection with respect to discrete lines

This method was presented by Andres [7]. This approach was designed to leave invariant discrete lines after reflections. The reflection of a point is computed by simply identifying its position with respect to the point of intersection between the discrete line and its perpendicular discrete line. Again, this approach is one-one point mapping thus bijective.

2.3 Bijective digitized reflections and rotations

We focus in this subsection on the approach that follows (b). First, let us recall the necessary and sufficient condition for a digitized rotation and a digitized reflection to be bijective. This condition provides the subsets

- R^k such that $\forall R_\alpha \in R^k$, $\mathcal{D} \circ R_\alpha$ is bijective for digitized rotations,
- H^k such that $\forall H_{\mathbf{m}} \in H^k$, $\mathcal{D} \circ H_{\mathbf{m}}$ is bijective for digitized reflections (\mathbf{m} being the normal vector of the hyperplane used for the reflection).

We start by recalling the characterization of 2D bijective digitized rotation with angle $\alpha \in [0, \frac{\pi}{2}]$ made by Nouvel and Rémila [1]:

$$R^k = \left\{ \cos(\alpha) = \frac{2k+1}{2k^2+2k+1}, \sin(\alpha) = \frac{2k^2+2k}{2k^2+2k+1}, k \in \mathbb{Z}^+ \right\}. \quad (1)$$

More recently, Roussillon and Coeurjolly [11] expressed the bijectivity condition in the complex plane by the Gaussian integers $\gamma \in \mathbb{Z}[i]$ (ring of Gaussian integers) as follows:

$$R^k = \left\{ \frac{\gamma \cdot \gamma}{\sqrt{(\gamma \cdot \gamma^*)}} \mid \gamma = (k+1) + ki, k \in \mathbb{Z}^+ \right\}. \quad (2)$$

In order to express the bijectivity condition of digitized reflections, Breuils et al. [8] used the Geometric Algebra \mathbb{G}^2 with basis vectors $\mathbf{e}_1, \mathbf{e}_2$. The resulting subset H^k of bijective digitized reflections is

$$H^k = H_1^k \cup H_2^k \cup H_3^k \cup H_4^k, \quad (3)$$

where

$$\begin{aligned} H_1^k &= \{\mathbf{m} \in \mathbb{G}^2, \mathbf{m} = -k\mathbf{e}_1 + (k+1)\mathbf{e}_2\}, H_2^k = \{\mathbf{m} \in \mathbb{G}^2, \mathbf{m} = -(k+1)\mathbf{e}_1 + k\mathbf{e}_2\}, \\ H_3^k &= \{\mathbf{m} \in \mathbb{G}^2, \mathbf{m} = -\mathbf{e}_1 + (2k+1)\mathbf{e}_2\}, H_4^k = \{\mathbf{m} \in \mathbb{G}^2, \mathbf{m} = -(2k+1)\mathbf{e}_1 + \mathbf{e}_2\}. \end{aligned} \quad (4)$$

Note that the reflection \mathbf{p}' of a point $\mathbf{p} \in \mathbb{R}^2$ with respect to a hyperplane of normal vector $\mathbf{m} \in \mathbb{G}^2$ can be written as

$$\mathbf{p}' = -\mathbf{m}\mathbf{p}\mathbf{m}^{-1} = \mathbf{p} - 2\frac{\mathbf{m} \cdot \mathbf{p}}{\mathbf{m} \cdot \mathbf{m}}\mathbf{m}, \quad (5)$$

where $\mathbf{m}\mathbf{p} = \mathbf{m} \cdot \mathbf{p} + \mathbf{m} \wedge \mathbf{p}$ represents the geometric product between the vector \mathbf{m} and \mathbf{p} . Note, that the geometric product acts on basis vectors as follows

$$\mathbf{e}_i\mathbf{e}_j = \begin{cases} 1 & \text{if } i = j \\ -\mathbf{e}_{ji} & \text{otherwise} \end{cases} \quad \text{and} \quad \mathbf{e}_{ij}\mathbf{e}_k = \begin{cases} \mathbf{e}_i & \text{if } j = k \\ -\mathbf{e}_j & \text{if } i = k \end{cases}. \quad (6)$$

where \mathbf{e}_{ij} is called a basis bivector. In geometric algebra [12], a rotation can be expressed as the composition of two reflections. Assuming \mathbf{m}, \mathbf{n} be the two unit normal vectors of the reflections, the rotation is expressed as

$$\mathbf{x}' = (\mathbf{nm})\mathbf{x}(\mathbf{nm})^{-1} = (\cos \frac{\alpha}{2} + \sin \frac{\alpha}{2} \mathbf{e}_{12})\mathbf{x}(\cos \frac{\alpha}{2} - \sin \frac{\alpha}{2} \mathbf{e}_{12}). \quad (7)$$

Furthermore, the composition of reflections with normal vectors $\mathbf{m}_1, \mathbf{m}_2, \dots, \mathbf{m}_n$ is expressed as the reflection induced by the hyperplane defined by the geometric product of the normal vectors

$$\mathbf{m}_1\mathbf{m}_2 \cdots \mathbf{m}_n. \quad (8)$$

As a consequence, if n is even and each normal vector is a unit vector then the above geometric product acts as a rotation on a point \mathbf{x} .

3 Composition of bijective digitized reflections

These characterisations lead to bijective digitized rigid transformations. However, the resulting angular distribution of both R^k and H^k is far from being dense, see Figure 2. When computing a rotation by an angle not in R^k and H^k , one option would be to consider the nearest bijective rotation or reflection. However, this leads to low quality transformations (*e.g.* mean squared distance error between rotated grid points and the original subset of the grid). Since the composition of an even number of reflections results to a rotation, an alternative is to compose bijective digitized reflections, for instance 4 of them, to approximate a given target rotation angle. More precisely, we aim at constructing a look-up table that associates, to some prescribed rotation angles, the sequence of reflections that minimises some error metrics.

3.1 Candidate set construction and duplicates

First of all, let us fix $k = k_{\max}$ and compute the composition of the elements of $H^{k_{\max}}$. The set of composition of 4 bijective digitized reflections $C^{k_{\max}}$ is expressed as

$$C^{k_{\max}} = \{(\mathbf{m}_1, \mathbf{m}_2, \mathbf{m}_3, \mathbf{m}_4) \mid \mathbf{m}_1, \mathbf{m}_2, \mathbf{m}_3, \mathbf{m}_4 \in H^{k_{\max}}\}. \quad (9)$$

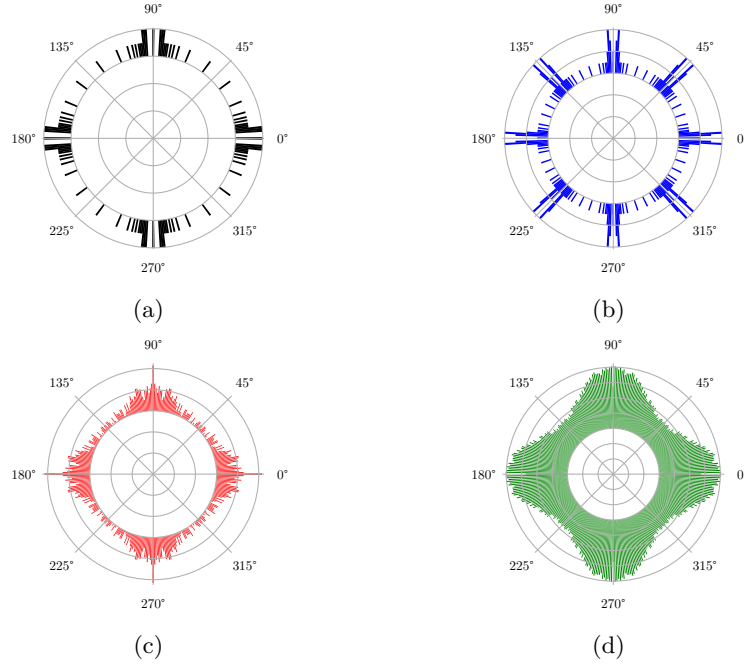


Fig. 2: Angular density distributions of bijective digitized rotations colored in black (a), bijective digitized reflections colored in blue (b), the composition of 2 bijective digitized reflections colored in red (c) and the composition of 4 bijective digitized reflections colored in green (d) .

From our experiments, we do not compose more reflections than 4 since the maximum angular uncertainty is already lower than one degree 0.00015 rad for $k_{\max} = 15$. Figures 2c and 2d show the two normalised angular histograms of $C^{k_{\max}}$ for 2 and 4 reflections.

Remark 1. $\text{card}(C^{k_{\max}}) = (4k_{\max})^4$.

Proposition 1. $R^{k_{\max}} \subset C^{k_{\max}}$.

Proof. Let $\gamma = (k + 1) + ki \in R^{k_{\max}}$ and since the subalgebra composed of the scalar and bivector $\mathbb{R} \oplus \wedge^2 \mathbb{R}^2$ is isomorphic to the complex numbers $((\mathbf{e}_{12})^2 = i^2 = -1)$, then $\exists \mathbf{m}_1, \mathbf{m}_2 \in H^{k_{\max}}, \gamma = \mathbf{m}_1 \mathbf{m}_2$. For instance, choose $\mathbf{m}_1 = \mathbf{e}_1, \mathbf{m}_2 = (k + 1)\mathbf{e}_1 + k\mathbf{e}_2$. Their product is

$$\mathbf{m}_1 \mathbf{m}_2 = (\mathbf{e}_1)((k + 1)\mathbf{e}_1 + k\mathbf{e}_2) = (k + 1) + k\mathbf{e}_{12} \in R^{k_{\max}} .$$

□

We also observe that several compositions of bijective digitized reflections result in the same rotation angle. This becomes critical if the value of k_{\max}

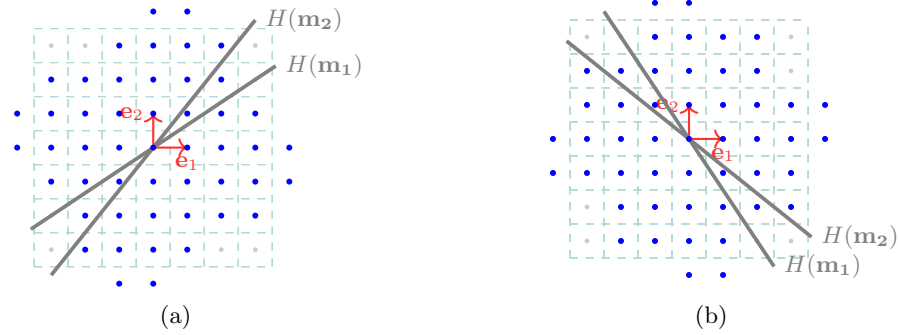


Fig. 3: Composition of 2 bijective digitized reflections $\mathbf{m}_1, \mathbf{m}_2$. (a) $\mathbf{m}_1 = -2\mathbf{e}_1 + 3\mathbf{e}_2$, $\mathbf{m}_2 = -5\mathbf{e}_1 + 4\mathbf{e}_2$. (b) $\mathbf{m}_1 = 4\mathbf{e}_1 + 5\mathbf{e}_2$, $\mathbf{m}_2 = 3\mathbf{e}_1 + 2\mathbf{e}_3$. The angle between the normal vectors in (a) and (b) are the same whereas their digitizations (points in blue) are different, for example $4\mathbf{e}_1 + \mathbf{e}_2$ is in the lattice of (b) but not (a).

increases (with $k_{\max} = 15$, $\text{card}(C^{k_{\max}}) = 40.10^6$). In order to reduce overhead associated to the storage of this table, the duplicates must be removed. This involves sorting $C^{k_{\max}}$ by increasing angle of the resulting rotation. Furthermore, it is important to note that two compositions resulting in the same angle might have different digitizations, see Figure 3. Thus, for each angle α , we choose

$$\text{RefRot}[\alpha] := \arg \min_{(\mathbf{m}_1, \mathbf{m}_2, \mathbf{m}_3, \mathbf{m}_4) \in C^{k_{\max}}} \|\Pi_{i=1}^n (\mathcal{D} \circ -\mathbf{m}_i \mathbf{p} \mathbf{m}_i^{-1}) - R_\alpha(\mathbf{p})\|_\infty. \quad (10)$$

Note that $\Pi_{i=1}^n \mathbf{m}_i = \cos(\frac{\alpha}{2}) + \sin(\frac{\alpha}{2})\mathbf{e}_{12}$. Furthermore, in practice, we choose $\mathbf{p} \in D_p$ where $D_p = \mathbb{Z}^2 \cap [-100, 100]^2$. Finally, with $k_{\max} = 15$, we reduce $\text{card}(C^{k_{\max}})$ to 10^5 compositions instead of 40.10^6 before.

3.2 Rotation angle to the most accurate bijective composition

Given a target rotation angle α and $C^{k_{\max}}$ sorted and without duplicates, we seek for $C_i^{k_{\max}} \in C^{k_{\max}}$ that best approximates $R_\alpha(\mathbf{p})$. Firstly, since $C^{k_{\max}}$ is sorted by ascending angle, finding $C_i^{k_{\max}}$ with a resulting angle α is a binary search operation. However, this element is not necessarily the composition that is the most accurate, meaning that minimizes the distance with the Euclidean rotation $R_\alpha(\mathbf{p})$. For instance, let us consider a target rotation angle ϵ near 0, there might be a composition of 4 bijective reflections resulting in ϵ whereas the most accurate one is simply the composition of the two trivials reflections with normal vectors $\mathbf{m}_1 = \mathbf{m}_2 = \mathbf{e}_1$. To address this issue, we start by computing the K compositions of bijective digitized reflections nearest to $C_i^{k_{\max}}$ where $C_i^{k_{\max}}$ is the composition of bijective digitized reflections whose resulting angle is the closest to the target angle. We call this subset $NN(C_i^{k_{\max}}, \alpha)$. We then seek for the composition of digitized reflections that minimizes either

$$\widetilde{R}_\alpha = \arg \min_{(\mathbf{m}_1, \mathbf{m}_2, \mathbf{m}_3, \mathbf{m}_4) \in NN(C_i^{k_{\max}}, \alpha)} \|\Pi_{i=1}^4 (\mathcal{D} \circ -\mathbf{m}_i \mathbf{p} \mathbf{m}_i^{-1}) - R_\alpha(\mathbf{p})\|_\infty \quad (11)$$

or

$$\widetilde{R}_\alpha = \arg \min_{(\mathbf{m}_1, \mathbf{m}_2, \mathbf{m}_3, \mathbf{m}_4) \in NN(C_i^{k_{\max}}, \alpha)} \|\Pi_{i=1}^4(\mathcal{D} \circ -\mathbf{m}_i \mathbf{p} \mathbf{m}_i^{-1}) - R_\alpha(\mathbf{p})\|_2. \quad (12)$$

3.3 Computational complexity

The computational cost of sorting the $C^{k_{\max}}$ and remove duplicates is

$$O(\max(\text{card}(D_p), \text{card}(C^{k_{\max}})) \log(\text{card}(C^{k_{\max}}))). \quad (13)$$

Note that $\text{card}(D_p) = 201 \times 201$. Since this latter operation can be computationally expensive, we choose to pre-compute $C^{k_{\max}}$. In practical implementation, we go a step further by precomputing the table of the most accurate composition of bijective digitized reflections for each angle and for the points of D_p . It is worth mentioning this table remains reusable as the number of points increases. Therefore, if we consider an image of size $N \times N$, the complexity of the approach is the complexity of applying bijective digitized reflections to each point of the image. Thus, the overall complexity is $O(N^2)$. Figure 6 shows 2 figures of the composition of digitized reflections applied to an image. The resulting implementation of this approach is available in DGtal [13].

4 Bijective rotation by circles

We build a bijective approximation of a rotation by decomposing the plane into concentric digital circles around the center of rotation. The points along each digital circle are sorted according to the angle they form with the center of rotation and the x -axis. Then the global transformation is constructed by mapping circles onto themselves, shifting the points according to the desired angle α .

More precisely, assuming the origin of the frame lies at the center of rotation, let $C^r := \{p \in \mathbb{Z}^2, r \leq \|p\|_2 < r+1\}$. It is clear that $(C^r)_{r \in \mathbb{Z}, r \geq 0}$ forms a partition of \mathbb{Z}^2 . We then sort the points of each circle C^r according to their angle with the x -axis: let $(C_i^r)_{i=0, \dots, n^r-1}$ be the induced sequence of points, where n^r is the cardinal of C^r . We have thus $\forall 0 \leq i < j < n^r, \angle(C_i^r O x) < \angle(C_j^r O x)$. Denoting by $\lfloor \cdot \rfloor$ the nearest integer rounding operator, we define the *rotation along circles* R_α^C of angle α as:

$$\forall p \in \mathbb{Z}^2, R_\alpha^C(p) = q, \quad \text{with} \quad \begin{cases} p = C_i^r, q = C_j^r \\ \text{and } j = (i - \lfloor \frac{\alpha}{2\pi} n^r \rfloor) \pmod{n^r}. \end{cases}$$

This transformation is clearly bijective: it maps the points of a circle onto the same circle, and the shift of indices is a one-one mapping. This transformation also preserves circles and minimizes the radial error in some sense.

From a computational point of view, rotating a whole image of size $N \times N$ takes a time $\Theta(N^2)$. It suffices to proceed circle by circles, each shift takes a

time linear in the number of points of the circle. If one is interested in rotating just one point $p = C_i^r$, the complexity is then $O(\log N)$: it takes $O(1)$ to find the correct circle radius r , then $O(\log N)$ worst case to find the index i of p in the sequence, and finally $O(1)$ to get the shifted point.

5 Optimal Transport method

In recent years, Optimal Transport (OT for short) has become a key mathematical framework for manipulating generalized probability density functions (e.g. [14]). The most general way to describe the interest of OT is that it allows quantifying meaningfully how costly it is to move masses from a generalized probability density function to another one, so-called the Wasserstein distance. Depending on the nature of the measures, discrete-to-discrete, semi-discrete, or continuous-to-continuous, a huge literature exists on numerical methods to efficiently solve OT problems [15,16]. When dealing with discrete measures with unit masses, the OT problem boils down to an optimal assignment problem: given two sets of points $X = \{x_i\}_n$ and $Y = \{y_i\}_n$ in \mathbb{R}^d , and a cost function $c : \mathbb{R}^d \times \mathbb{R}^d \rightarrow \mathbb{R}^+$, we are looking for the permutation σ in $\{1..n\}$ such that

$$\sum_{i=1}^n c(x_i, y_{\sigma(i)})$$

is minimal. Back to our setting, if X and Y are two discrete sets and c the squared Euclidean distance, the OT approach allows us to construct a bijective map $X \rightarrow Y$ that minimizes the mean squared l_2 error between X and Y . If X is a finite disk of \mathbb{Z}^d and $T \in E(d)$ any continuous rotation, one can define the OT variant of T (e.g. OT based rotations) as the optimal assignment between X and $T(X)$ for the (squared) l_2 cost. On the computational side, the Hungarian method can be used to compute the optimal assignment (see for example [15]) with a $O(n^4)$ computational cost, for n the number of pixels. In this paper, we rely on a fast network simplex algorithm [17,18]. The worst-case computational cost remains highly polynomial in n (i.e. $O(N^8)$ for an image $N \times N$), but the bound is not reached in practice. To get an idea of computation times, rotating a 100×100 image takes several minutes on an Apple M2 processor.

6 Optimal Transport by circles

Since the OT of an image is very costly and impracticable for nowadays image resolutions, we construct a new bijective transformation by mixing rotation by circles and OT. More precisely, for a constant $k \geq 2$, we group concentric circles C^r by k -tuples, leaving only C^0 alone. We thus build digital sets D^i that are grouped concentric circles:

$$D^0 := C^0 \quad \forall i \geq 0, D^{i+1} := \bigcup_{j=1}^k C^{k^i+j}. \quad (14)$$

Then, given a rotation T_α of angle α , for each circular ring D^i , we perform the optimal transport between $T_\alpha(D^i)$ and D^i to find the best (as of L_2) bijective rotation within each ring. Note that the computational cost is now $N \times O(k^4 N^4)$, since the number of points within a ring is proportionnal to kN . Finally, we can build a look-up table for a fixed number of angles (like 360) that gives the assignment for each ring.

7 Experimental results and discussions

We consider the following bijective approximations approaches

- Quasi-shears (QSH)
- Rotation as the composition of discrete line reflections (CDLR)
- Bijective digitized rotations (BROT)
- Composition of bijective digitized reflections (CBDR)
- Bijective rotation by circles (RBC)
- Optimal transport (OT)
- Optimal transport by circles (OTC)

The next subsections present the result of these approaches both in terms of computational complexity and accuracy.

7.1 Computational complexity

We evaluate the computational complexity of rotating a whole image of size $N \times N$. As for the quasi-shear approach, we consider the algorithm of [4] presented in page 313, namely `Final_QSR`. Applying a shift to a point is a constant time algorithm thus the complexity is $O(N^2)$. Concerning the rotation as the composition of discrete line reflections approach, we rely on Algorithm 1 of [7]. The function $X(y)$ defined in line 2 computes a rounding operation and this operation is a constant-time operation. The table 1 summarizes the complexity of both the image transformation and the table precomputation for the methods presented in this paper.

7.2 Accuracy

The accuracy of each method is given in terms of Euclidean distance between the Euclidean rotation and the digital approximation method. More precisely, we compute both the L_2 and L_∞ norms of the error between the Euclidean rotation and the approximation method. As for method CDLR, we improve it by modifying Algorithm 1 [7], where we choose the first reflection such that the L_∞ norm of the error is minimized. Figures 4 and 5 displays respectively the L_2 -error and L_∞ -error for each method as a function of the angle of rotation.

Overall, bijective rotations (BROT) constitute the worst trade-off, because their angle density is too scarce. Quasi-shears (QSH) have quite regular errors but remain less interesting than a few other methods. Composition of discrete

Method	QSH	CDLR	BROT	CBDR	RBC	OT	OTC-k		
Image transf.	$\Theta(N^2)$	$\Theta(N^2)$	$\Theta(N^2)$	$\Theta(N^2)$	$\Theta(N^2)$	$O(N^8)$	$O(N^2 \log(N))$		
Precomp.	n.a.	n.a.	n.a.	Eq. (13)	$O(N^2)$	n.a.	$O(k^3 N^5)$		
Image transf. (ms)	2.7	43.5	3.8	3.8	3.5		OTC-2 $3.6 \cdot 10^5$	OTC-3 $7.2 \cdot 10^5$	OTC-4 $12.7 \cdot 10^5$
Precomp. (ms)	0	0	0	5300	20	0	time 2	time 3	time 4

Table 1: For the main approaches, the first two lines describe the time complexity and the precomputation time complexity to apply each bijective transformation method to a $N \times N$ image. The remaining lines present both the time (ms) to transform a 201×201 image (Image transf.) as well as the precomputation time required for the same image (Precomp.). For CBDR, we choose $kmax = 15$. Methods proposed in this paper are emphasized in bold font. For OTC- k , k stands for the width of each ring (see Eq. (14)).

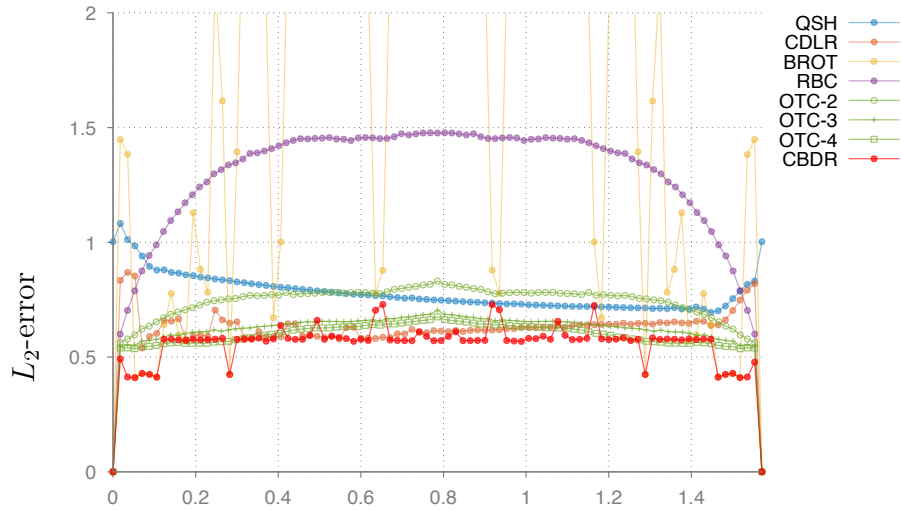


Fig. 4: Plots of L_2 -errors for the different bijective transformations as a function of the angle (90 angles between $[0, \frac{\pi}{2}]$), y -range is between 0 and 2 pixels.

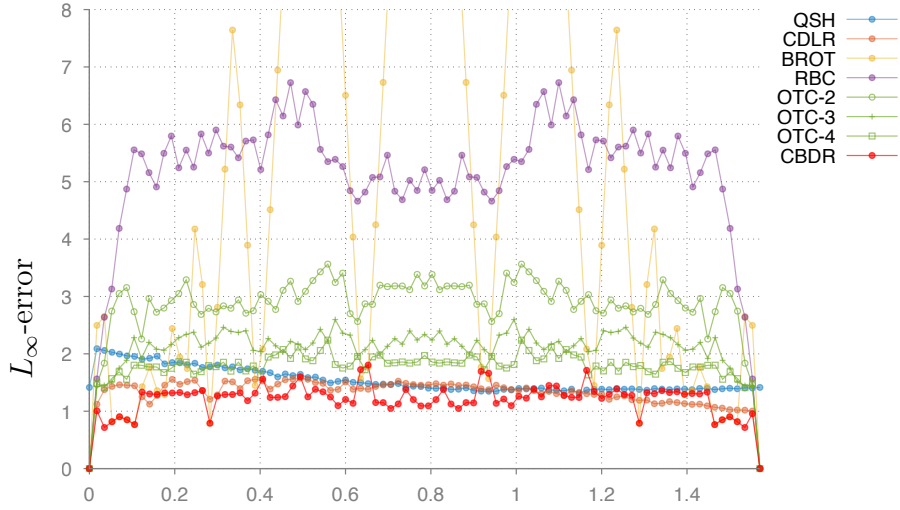


Fig. 5: Plots of L_∞ -errors for the different bijective transformations as a function of the angle (90 angles between $[0, \frac{\pi}{2}]$), y -range is between 0 and 8 pixels.

line reflections (CDLR) is among the best methods (both in worst-case or average error). Rotations by circles (RBC) induce quite large errors (especially in worst-case). However their optimal transport extensions (OTC- k) present lower and lower errors as the width k of each ring is increased. Indeed method OTC with rings of width 4 is only outperformed by CBDR, and not for all angles. Increasing the ring width would probably induce the method with lowest average error, but its precomputation is very costly (several days). Last, compositions of bijective reflections (CBDR) provide generally the best results on average and in worst-case, while staying fast to compute. Figure 6 in appendix gives a visual comparison of each approximation method for both the worst case and a fixed angle (61°). For both the worst case and the fixed angle, we also show the L2 norm error field with respect to the Euclidean rotation. Note that all implementations are available in DGtal [13]³.

8 Conclusion

In this paper, we presented multiple approaches for handling bijective rigid transformations and conducted a comparative analysis against state-of-the-art methods. Our experimental results highlight the performances of both optimal transport with circles and the composition of bijective digitized reflections. Extending to 3D the proposed approximation methods is one of our perspectives. A major

³ <https://github.com/DGtal-team/DGtal>

problem with the extension is the computational complexity. Furthermore, in 3D, the angular density of bijective digitized rotations and reflections is even sparser than in 2D, see [2]. Finally, we are also interested in investigating other mixes of optimal transport and bijective approximation approach.

Acknowledgments

This work is supported by both the Savoie Mont-Blanc University (TRDRECAL project) and the French National Research Agency (StableProxies project, ANR-22-CE46-0006).

References

1. Bertrand Nouvel and Eric Rémila. Characterization of Bijective Discretized Rotations. In *International Workshop on Combinatorial Image Analysis*, pages 248–259. Springer, 2004.
2. Stéphane Breuils, Yukiko Kenmochi, Eric Andres, and Akihiro Sugimoto. Conjecture on characterisation of bijective 3D digitized reflections and rotations. In *International Workshop on Empowering Novel Geometric Algebra for Graphics and Engineering*, pages 41–53. Springer, 2022.
3. Kacper Pluta, Tristan Roussillon, David Coeurjolly, Pascal Romon, Yukiko Kenmochi, and Victor Ostromoukhov. Characterization of bijective digitized rotations on the hexagonal grid. *Journal of Mathematical Imaging and Vision*, 60(5):707–716, 2018.
4. Eric Andres. The Quasi-Shear rotation. In Serge Miguet, Annick Montanvert, and Stéphane Ubéda, editors, *Discrete Geometry for Computer Imagery*, pages 307–314, Berlin, Heidelberg, 1996. Springer Berlin Heidelberg.
5. Hans-Georg Carstens, Walter A Deuber, Wolfgang Thumser, and Elke Koppenrade. Geometrical bijections in discrete lattices. *Combinatorics, Probability and Computing*, 8(1-2):109–129, 1999.
6. Tommaso Toffoli and Jason Quick. Three-dimensional rotations by three shears. *Graphical Models and Image Processing*, 59(2):89–95, 1997.
7. Eric Andres, Mousumi Dutt, Arindam Biswas, Gaelle Largeteau-Skapin, and Rita Zrou. Digital Two-Dimensional Bijective Reflection and Associated Rotation. In *Discrete Geometry for Computer Imagery*, pages 3–14. Springer International Publishing, 2019.
8. Stéphane Breuils, Yukiko Kenmochi, and Akihiro Sugimoto. Visiting bijective digitized reflections and rotations using geometric algebra. In *International Conference on Discrete Geometry and Mathematical Morphology*, pages 242–254. Springer, 2021.
9. Nicolas Passat, Phuc Ngo, Yukiko Kenmochi, and Hugues Talbot. Homotopic affine transformations in the 2D cartesian grid. *Journal of Mathematical Imaging and Vision*, 64(7):786–806, 2022.
10. Eric Andres. *Cercles Discrets et Rotations Discrètes*. PhD thesis, Université Louis Pasteur, Strasbourg, France, 1992.
11. Tristan Roussillon and David Coeurjolly. Characterization of bijective discretized rotations by Gaussian integers. Research report, LIRIS UMR CNRS 5205, 2016.

12. Leo Dorst, Daniel Fontijne, and Stephen Mann. *Geometric Algebra for Computer Science, An Object-Oriented Approach to Geometry*. Morgan Kaufmann, 2007.
13. DGtal: Digital geometry tools and algorithms library.
14. Cédric Villani. *Optimal transport: old and new*, volume 338. Springer, 2009.
15. Gabriel Peyré, Marco Cuturi, et al. Computational optimal transport: With applications to data science. *Foundations and Trends in Machine Learning*, 11(5-6):355–607, 2019.
16. Rémi Flamary, Nicolas Courty, Alexandre Gramfort, Mokhtar Z. Alaya, Aurélie Boisbunon, Stanislas Chambon, Laetitia Chapel, Adrien Corenflos, Kilian Fatras, Nemo Fournier, Léo Gautheron, Nathalie T.H. Gayraud, Hicham Janati, Alain Rakotomamonjy, Ievgen Redko, Antoine Rolet, Antony Schutz, Vivien Seguy, Danica J. Sutherland, Romain Tavenard, Alexander Tong, and Titouan Vayer. Pot: Python optimal transport. *Journal of Machine Learning Research*, 22(78):1–8, 2021.
17. Nicolas Bonneel, Michiel van de Panne, Sylvain Paris, and Wolfgang Heidrich. Displacement Interpolation Using Lagrangian Mass Transport. *ACM Transactions on Graphics (SIGGRAPH ASIA 2011)*, 30(6), 2011.
18. Nicolas Bonneel. Fast network simplex for optimal transport, https://github.com/nbonneel/network_simplex, 2018.

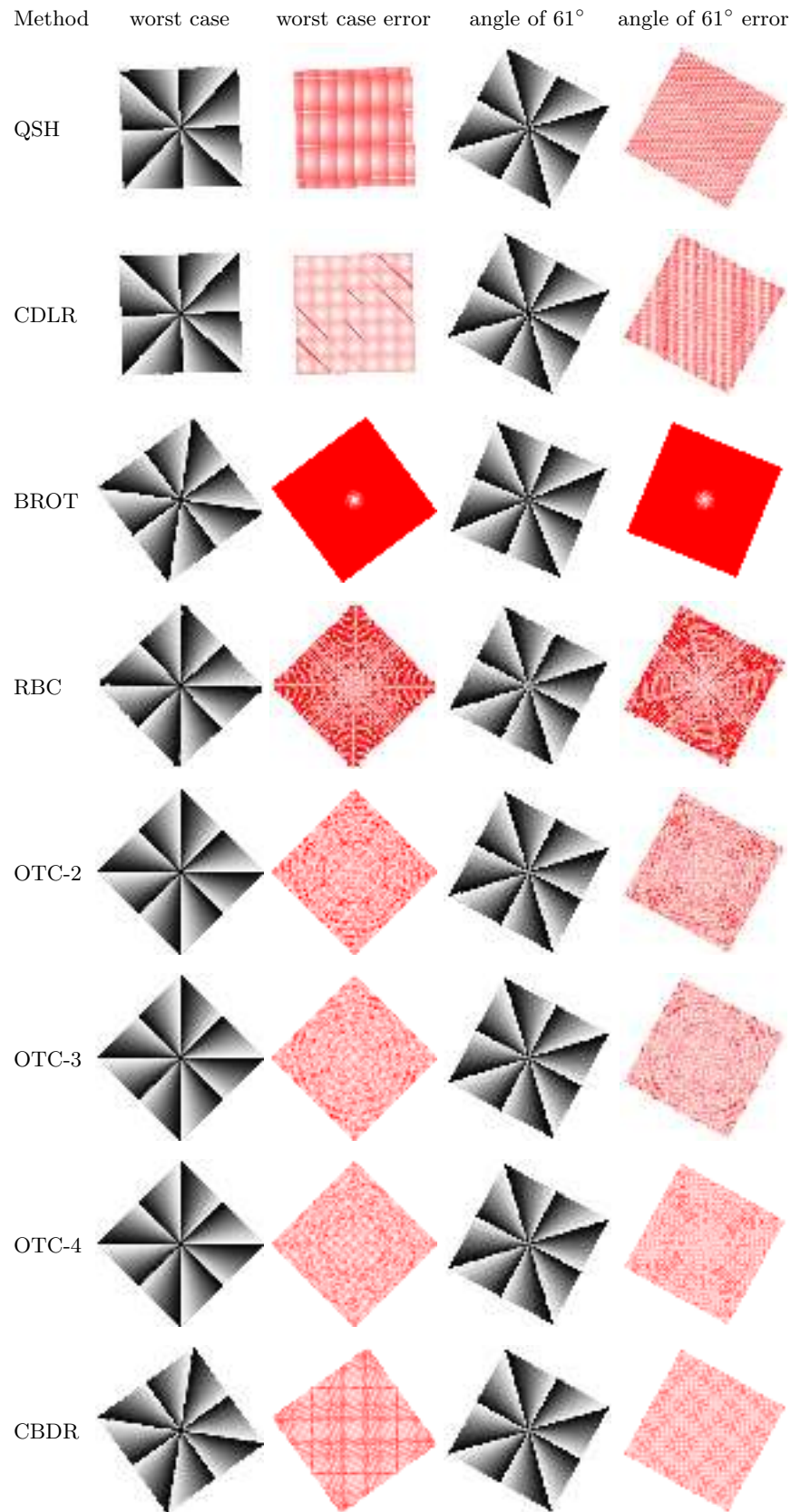


Fig. 6: Comparison of worst case results, norm of the error with respect to the Euclidean rotation (red), and 61-degree rotation for each approximation method